Adsorption of atmospherically relevant gases at the air/water interface: Free energy profiles of aqueous solvation of N_2, O_2, O_3, OH, H_2O, HO_2, and H_2O_2

Robert Vácha,[1] Petr Slavíček,[1#] Martin Mucha,[1] Barbara J. Finlayson-Pitts,[2] and Pavel Jungwirth[1*]

[1]*Institute of Organic Chemistry and Biochemistry, Academy of Sciences of the Czech Republic and Center for Complex Molecular Systems and Biomolecules, Flemingovo nam. 2, 16610 Prague 6, Czech Republic*

[2]*Department of Chemistry, University of California, Irvine, CA 92697-2025, USA*

[*]To whom correspondence should be addressed. E-mail: pavel.jungwirth@uochb.cas.cz

[#]Present address: Department of Chemistry, University of Illinois, Urbana, IL 61801, USA

Abstract

Free energy profiles associated with moving atmospheric gases or radicals across the air/water interface were calculated as potentials of mean force by classical molecular dynamics simulations. With the employed force field the experimental hydration free energies are satisfactorily reproduced. The main finding is that both hydrophobic gases (nitrogen, oxygen, and ozone), as well as hydrophilic species (hydroxyl radical, hydroperoxy radical, or hydrogen peroxide) have a free energy minimum at the air/water interface. As a consequence, it is inferred that atmospheric gases, with the exception of water vapor, exhibit enhanced concentrations at

surfaces of aqueous aerosols. This has important implications for understanding heterogeneous chemical processes in the troposphere.

1. Introduction

The role of liquid aerosols, such as water microdroplets or aqueous sea salt particles, in the chemistry of the troposphere is being increasingly recognized.[1] The standard picture of aqueous aerosols as tropospheric "mini-reactors" involves the uptake of reactive gases, followed by diffusion and chemical reactions in the aerosol and release of the products back into the atmosphere. It has been shown recently, however, that important tropospheric reactions can take place at the surfaces of liquid aerosols. For example, measurements and modeling studies strongly indicate that the photochemical formation of molecular chlorine in the ozone containing marine boundary layer is primarily a heterogeneous process occurring at the air/water interface of aqueous sea salt aerosols.[2,3]

In order to quantify chemical processes occurring in liquid aerosols it is essential to know the atmospheric concentrations of the reactive gases and their solubilities. At low gas concentrations and reactivities the uptake into the liquid aqueous aerosols can be usually characterized via the corresponding Henry law constant, which is directly related to the hydration free energy of the particular gas.[4] Leaving aside cases where the concentration or reactivity of a solvated gas is high, the use of the Henry law constant can also be improper for reactions occurring at the surfaces of liquid aerosols. More precisely, it is by no means obvious that the concentration of a reactive gas monotonously switches at the air/water interface from the gas phase value to that in the aqueous bulk of the aerosols. As a matter of fact, it has been known for almost a century that the surface tension of water slightly decreases with increasing atmospheric

pressure, which can be interpreted via the Gibbs equation in terms of adsorption of nitrogen and/or oxygen at the aqueous surface.[5] The conditions under which one might expect deviations from Henry's law due to adsorption of a variety of species, particularly organics, on the surfaces of particles in the atmosphere have been discussed recently by Djikaev and Tabazadeh.[6]

In the present paper we investigate by means of molecular dynamics simulations the process of aqueous solvation of a series of atmospherically relevant gases including nitrogen, oxygen, ozone, hydroxyl radical, water vapor, hydroperoxy radical, and hydrogen peroxide. Solvation of OH and HO_2 in small and medium sized water clusters has been studied in the last years by means of ab initio quantum chemistry methods and infrared spectroscopy,[7-10] while the uptake of OH, O_3, and HO_2 at aqueous surfaces was most recently modeled within kinetic molecular dynamics studies.[11-13] Here, we evaluate the free energy profiles (i.e., the so called potentials of mean force[14,15]) associated with transporting the gas molecule across the extended air/water interface into the aqueous bulk, with emphasis on the behavior at the aqueous surface. We show that almost all these gases exhibit a surface free energy minimum and, consequently, a concentration enhancement at the air/water interface, which has important implications for heterogeneous tropospheric chemistry.

2. Computational Approach

For investigation of the aqueous solvation of atmospheric gases we used classical molecular dynamics (MD) simulations performed using the program package Gromacs 3.1.5.[16] For each of the gas species we calculated the potential of mean force (PMF), i.e., the free energy profile ΔG connected with moving the molecule from the gas phase through an aqueous slab back to the gas phase. From the free energy difference between points 1 and 2 at the path (e.g., in

the liquid, at the surface, or in the gas phase) one can evaluate the molecular concentration ratio of the host species at these points

$$\frac{c_1}{c_2} = e^{-\frac{\Delta G_{12}}{RT}} \tag{1}$$

If we take one point in the liquid and the other in the gas phase, the calculated ratio can be compared to the experimental Henry's law constant. Here, we adopt a definition, where the Henry's law constant is given as the concentration of a molecule in the liquid divided by its partial pressure in the gas phase:[4]

$$k_H = \frac{c_l}{p_g} \tag{2}$$

Henry's law can, however, be also written in dimensionless form as a ratio between molecular concentrations in the liquid and the gas phase:

$$k_H{}^{cc} = \frac{c_l}{c_g} \tag{3}$$

There is a simple relation between these two constants and the solvation free energy of the molecular species at infinite dilution:

$$k_H{}^{cc} = k_H \cdot RT = e^{-\frac{\Delta G_{solv}}{RT}} \tag{4}$$

Here, R is the universal gas constant, T stands for temperature, c_l and c_g are concentrations in the liquid and gas phases, k_H is the Henry's law constant, and ΔG_{solv} is the solvation free energy, which can be directly compared to our calculations. Note that the standard solvation free energies (at p_0 = 1 atm gas pressure and c_0 = 1 M concentration) differ from those corresponding to a single gas molecule (i.e., pertinent to the present simulations) by a factor $RT \ln(RTc_0/p_0)$.[17]

The values of Henry's law constants used in this study were taken from a compilation by Sander.[18]

3. Computational Details and Potential Parameters

Our system consisted of an atmospherically relevant molecule or radical (H_2O, N_2, O_2, O_3, HO, HO_2, or H_2O_2) and 215 water molecules. Water was placed in a rectangular cell with dimensions of 18.6 Å, 18.6 Å, and 388.6 Å and periodic boundary conditions were applied, yielding an infinite slab of a 20 Å thickness in the z-direction, possessing two air/water interfaces. An interaction cutoff of 9 Å was employed. The effect of long-range Coulomb interactions was accounted for using the smooth particle mesh Ewald summation.[19]

We employed the SPC/E model of water.[20] For the atmospheric molecules or radicals we chose among the existing parameterizations (or combinations thereof) those, which reproduced best the experimental hydration energies. The intermolecular force field parameters together with the relevant references[11,16,20,21] are summarized in Table I. The fractional charges and quadrupole moments were estimated at the MP2/aug-cc-pvtz level using the Gaussian03[22] program. In the cases of OH and ozone the charges were slightly increased to account for polarization effects and to better reproduce the solvation energies.

The PMF was calculated in a way schematically depicted in Fig. 1. A very heavy fictitious particle (X), defining a stationary point, was connected to the solute molecule (S) and to the center of mass of the water slab (CM). Both constraints act only in the z-direction normal to the slab surface, i.e., the resulting force has solely a z-component, posing thus no restriction to the movement of either slab or solute in the xy plane. The X-CM separation is kept constant,

fixing thus the water slab in space. By adjusting the X-S length we change the relative distance between the slab and the solute.

The whole simulation consisted of a series of two alternating processes: sampling and pulling. During each of the sufficiently long (1.5 ns) sampling periods, the X-S length was kept constant and the force has been measured and averaged over time. During each of the 20 ps pulling period, the length was varied by a total of 0.5 A. Thus, pulling was carried out sufficiently slowly to ensure that the system does not depart significantly from equilibrium. In about 80 such cycles the solute molecule was pulled through the whole slab and the profile of the mean force was obtained. Finally, integrating the force along the z-direction yielded the PMF, with a cumulative error (estimated from the slight asymmetry of the PMF curve with respect to the center of the slab) of ~0.3 kcal/mol.

4. Results and Discussion

4.1 General features of solvation free energy profiles

Before presenting separately the free energy profiles of each of the atmospheric molecules or radicals under study, we discuss first their general features. Fig. 2 shows such a typical PMF together with the corresponding force and water density profile. While the force exhibits a certain statistical noise, its integral, i.e., the PMF, is already a relatively smooth curve. The PMF is defined up to an arbitrary additive constant, which we chose such as to make the free energy equal to zero in the gas phase. It levels off in the bulk liquid at the value of the solvation free energy. Note also the two shallow minima at each of the two air/water interfaces. Ideally, the PMF should be perfectly symmetric with respect to the center of the slab, any asymmetries indicating thus systematic and convergence error margins of the actual calculation.

The PMF is shown again in detail, together with the corresponding concentration profile (see Eq. 1) in Fig. 3. The figure corresponds to a hydrophobic molecule, the free energy of which is lower in the gas phase than in the liquid and, consequently, its population in the aqueous bulk is lower that that in the gas phase. For a hydrophilic molecule or radical the situation is the opposite. The surface minima at the PMF correlate with enhancement of the host molecule concentration at the two air/water interfaces of the aqueous slab. As demonstrated in the following sections, this surface enhancement is a generic feature of all investigated host molecular and radical species at aqueous interfaces, except for water vapor itself. The three important free energy differences, the solvation (i.e., gas-to-liquid) free energy ΔG_{solv}, the gas-to-surface free energy difference ΔG_{gs}, and the surface-to-liquid free energy difference ΔG_{sl}, are also defined in Fig. 3. Only two of these values are independent, since $\Delta G_{solv} = \Delta G_{gs} + \Delta G_{sl}$.

4.2 Hydrophobic molecules

Out of the seven atmospheric gases under study, three are hydrophobic, i.e., their solvation free energy is positive. These are N_2, O_2, and O_3. Fig. 4a depicts the PMF for nitrogen together with the water density profile defining the extent of the aqueous slab. We see that simulations satisfactorily reproduce the solvation free energy of +2.5 kcal/mol derived from the experimental Henry's law constant. Curves exhibit surface minima implying an enhanced concentration of N_2 at the air/water interface compared to the gas phase. This surfactant behavior of nitrogen is consistent with the slight decrease of surface tension of water upon increasing the atmospheric pressure (by about 0.1 $mNm^{-1}atm^{-1}$).[5]

The PMF of molecular oxygen (see Fig. 4b) is similar to that of nitrogen. The employed force field reproduces well the experimental solvation free energy of +2.0 kcal/mol. As in the

previous case, a surface minimum develops with a depth of more than 0.5 kcal/mol, which corresponds at 300 K to a 240% enhancement of O_2 at the air/water interface compared to the gas phase. In agreement with previous studies,[23] a very weak barrier (of less than 0.25 kcal/mol) between the aqueous bulk and the surface region seems to develop at the PMF. Note, however, that the height of this barrier is probably within the error of the calculation.

Ozone is much less hydrophobic than the two dominant atmospheric gases with experimental solvation energy of +0.7- 0.9 kcal/mol, which is reproduced also by the present calculations (see Fig. 4c). At the same time, the surface minimum is deeper than in the case of O_2 or N_2, reaching 1.2 kcal/mol. This corresponds, at an ambient temperature, to a roughly seven-fold increase of ozone concentration at the air/water interface compared to the gas phase. This surfactant activity is in accord with the results of our previous dynamical study of ozone uptake at aqueous surfaces.[9] As in the case of molecular oxygen, a very weak (if any) barrier between the bulk region and the surface occurs on the PMF of ozone.

4.3 Hydrophilic molecules and radicals

The hydrophilic gases under investigation (the solvation free energy of which is negative) comprise hydroxyl radical, water vapor, hydroperoxy radical, and hydrogen peroxide. All these four gaseous species have a lower free energy in water than in the air, the hydration energy of the last two being even larger than that of a water molecule. Fig. 5a depicts the PMF for the OH radical. The experimental hydration energy of roughly -4 kcal/mol is reasonably well reproduced by the calculation. Also note the relatively very deep surface minimum of about 1.4 kcal/mol, corresponding to an order of magnitude concentration enhancement of OH at the surface

compared to the aqueous bulk. Results from the present PMF calculations thus support previous dynamical studies of the uptake of hydroxyl radical at aqueous surfaces.[9,10]

For water vapor, the hydration free energy from the present calculations agrees well with the chemical potential of H_2O of -6.3 kcal/mol (see Fig. 5b).[15] No appreciable (above statistical and systematic error) surface minimum is observed on the PMF – water is, of course, not a surfactant on water.[12]

A somewhat surprising fact is that even gases more hydrophilic than water vapor itself, such as hydroperoxy radical and hydrogen peroxide, develop a free energy minimum at the aqueous surface (see Figs. 5c and 5d). This is particularly remarkable for the HO_2 radical which exhibits a surface minimum of about half the magnitude of that of the less hydrophilic OH radical, while the surface free energy minimum of H_2O_2 is somewhat smaller. Finally, note that both in the case of hydroperoxy radical and hydrogen peroxide the hydration free energies derived from the experimental Henry's law constants are well reproduced by the present calculations.

4.4 Summary of calculations

The results of calculations are summarized in Table II, which shows for each of the gases under investigation their aqueous bulk concentration and its highest value in interfacial region, both normalized to the gas phase value. These values were obtained by converting the potentials of mean force into concentration profiles using Eq. 1 assuming temperature of 300 K. The table also shows the concentrations averaged over the surface peak area, together with the corresponding peak width. These mean surface concentrations are understandably lower than the

peak values, nevertheless the sizable surface enhancement, observed for most of the gases under study, pertains.

4.4 Implications for atmospheric chemistry

The enhancement of inorganic species at the air/water interface has some potentially important implications for reactions at the surfaces of particles in the atmosphere. In the troposphere, oxidation is well known to occur in the gas phase and in the bulk liquid phase of particles, fogs and cloud droplets.[1] The major oxidants are the hydroxyl radical and in coastal marine areas, atomic chlorine (primarily during the day), the nitrate radical (primarily at night) and ozone (both day and night). In addition, H_2O_2 and to a lesser extent organic hydroperoxides are important in the aqueous phase for the oxidation of dissolved SO_2, for example.

However, over the last decade, it has also been recognized that unique species and reactions of inorganics can occur at the air/water interface.[2,24-32] In addition, it has been proposed that organic compounds can be scavenged onto the surfaces of cloud droplets, resulting in higher net uptake of the organics than expected based on a Henry's law equilibrium.[6] The calculations presented above show that oxidants such as OH and O_3 are also expected to be enhanced in this region. The combination of oxidizable surface species along with enhanced concentrations of atmospheric oxidants at the interfaces of particles, fog and cloud droplets may play a significant role in the atmospheric processing of some organics as well as inorganic species.

For example, in recent field studies of clouds interacting with a plume from biomass burning, rapid oxidation of methanol to formaldehyde was observed.[33] This was much larger than that predicted from gas and bulk aqueous phase chemistry, and Tabazadeh and coworkers

suggested that it was due to heterogeneous processes. At a gas phase OH concentration[34] of 2×10^7 OH cm^{-3}, the equilibrium concentration of OH in the bulk phase of the cloud droplets would be 3.1×10^{-11} mol L^{-1} (using a Henry's law constant of 39 M atm^{-1}). Based on the present calculations of mean enhancement of OH at the interface by a factor of 8 (see Table II), the OH concentration in the interfacial region would be 2.5×10^{-10} mol L^{-1}. We take the interfacial width to be our calculated value of 6.9 A and the cloud surface area to be 6.3×10^{-3} cm^2 cm^{-3} as reported by Tabazadeh et al.[33] If the rate constant for oxidation of CH_3OH by OH in the bulk aqueous phase ($k = 8 \times 10^8$ M^{-1} s^{-1} at -5°C measured in the clouds)[35] is applicable to the interfacial region, then the observed rate of loss of gas phase CH_3OH from 36 ppb to 15 ppb in 3 min could be accomplished at the interface if the methanol surface coverage was ~ 0.4 % of a monolayer if there was no diffusion limitation for replenishing the methanol at the interface. While this surface coverage of methanol might not be expected for pure water droplets,[36] these clouds were heavily impacted by a biomass burning plume[33,34] which contains substantial amounts of organics both in the gas phase and in particles.[1] These would be expected to lead to an increased uptake of methanol and given the dense smoke plumes during these measurements, significant availability of the alcohol for oxidation at the interface is feasible.

A second example is the oxidation of polycyclic aromatic hydrocarbons (PAH) on the surfaces of particles, fogs and clouds. The vapor pressures of PAH are such that the smaller PAH exist totally in the gas phase, while the larger ones are in the particle phase; PAH of intermediate size and vapor pressures are semi-volatile and partition between the two phases.[1] For those that partition in whole or in part to particles, oxidation at the interface can be an important loss process in the atmosphere.

For example, Donaldson and coworkers[37,38] have shown that anthracene on water or aqueous solutions containing alcohols or acids is oxidized on exposure to gas phase O_3. The kinetics suggests that the mechanism involves the initial adsorption/desorption of ozone followed by oxidation of anthracene by the surface-adsorbed O_3 in a Langmuir-Hinshelwood type of process. Donaldson and coworkers[38] report that at 50 ppb O_3, the effective reaction probability is in the range of $(0.2 - 3) \times 10^{-7}$ depending on the composition of the underlying solution. For an air parcel containing 10^4 particles of 1 μm diameter per cm^3 of air, the loss of anthracene at the surface would be 3.5×10^3 molecules per cm^3 of air per second if the surface coverage of the anthracene is 1%. This can be compared to the gas phase rate of oxidation calculated to be 9×10^2 anthracene per cm^3 of air per second by OH (taken as 5×10^6 cm^{-3})[1] for an initial gas phase anthracene concentration of 1×10^7 cm^{-3}. One reason for the unusually rapid oxidation of anthracene observed by Donaldson and coworkers[38] at the interface may be enhancement of ozone in the interfacial which the present calculations suggest is about an order of magnitude compared to its bulk concentration. While the coverage of anthracene on particles in air is not known, it is likely that there will be cases such as biomass plumes (discussed above for methanol) and organics present on the surfaces of urban and sea salt particles,[39,40] that may lead to enhanced uptake of other organics such as the PAH.

A further potential consequence of the enhancement of O_3 in the interface region is increased production of OH and OH precursors such as H_2O_2 by photolysis of O_3.[1] When combined with the enhancement at the interface of other OH photochemical sources such as the nitrate ion,[41] the potential for increased oxidative capacity at the surface of particles, fogs and clouds is even more evident.

Clearly, the relative importance of gas, bulk liquid phase and interface oxidations will depend on a number of factors such as its gas phase concentrations, Henry's law constants and the surface coverage of the organic. For example, while napthalene has been reported to be enhanced at the air/water interface,[42] its high vapor pressure[1] is such that oxidation at the interface or in the bulk of particles cannot compete with the gas-phase oxidation by OH. However, for less volatile compounds, the gas phase processes become less important and the interface chemistry becomes relatively more so.

Finally, not all oxidants are significantly enhanced at the surface. For example, the present studies suggest that H_2O_2 is only increased in the interfacial region by ~ 50% compared to the bulk. Hydrogen peroxide is known to be a major aqueous phase oxidant for SO_2 [known as S(IV)] dissolved in fogs and clouds in the atmosphere.[1] The lack of a substantial increase in the predicted concentration of H_2O_2 at the interface is consistent with the experimental observation[43] that a surface reaction of H_2O_2 with SO_2 does not appear to be important compared to oxidation in the bulk, despite the existence of a S(IV) surface complex.[24,26,29,30]

In short, while our understanding of the importance of oxidations at the air/water interface of particles, fogs and clouds is in its infancy, the present calculations of enhanced oxidant concentrations in the interfacial region suggest that it is an area that should be pursued further.

Conclusions

We have calculated by means of molecular dynamics simulations the potentials of mean force connected with moving an atmospherically relevant molecule or radical (N_2, O_2, O_3, OH,

H_2O, HO_2, or H_2O_2) through an aqueous slab. The hydration free energies, as inferred from the experimental Henry's law constants, are well reproduced by the simulations. The present calculations indicate that the propensity of gaseous molecules and radicals for the air/water interface is a generic effect, present for both hydrophobic and hydrophilic species (with the only exception of water vapor itself). Out of the three phases involved (gas, liquid, and interface) the gaseous hosts thus have the highest concentration at the aqueous surface with a population enhancement with respect to the second most populated phase ranging from ~80 % (e.g., for N_2) to a factor of ~10 (e.g., for OH). The surface enhancement of atmospherically relevant gases has possible important consequences for heterogeneous atmospheric chemical processes occurring on aqueous aerosols and should be thus considered when interpreting the results of field measurements as well as in tropospheric models.

Acknowledgement

Support from the Czech Ministry of Education via a grant No. ME644 and from the US-NSF (grant CHE-0209719) is gratefully acknowledged. Part of the work in Prague has been completed within the framework of research project Z4 055 905. We thank Doug Tobias, Martina Roeselova, John Vieceli, Robert Yokelson, and Azadeh Tabazadeh for valuable discussions. We are also grateful to D. J. Donaldson for helpful discussions and for sharing preprints prior to publication.

Table I: Force field parameters.

		σ[Å]	ε[kcal/mol]	charge distribution	reference
N_2		4.201	0.1973	-1.740DÅ (quadrupole)	[21]
O_2		2.955	0.2029	-0.8081DÅ (quadrupole)	[16]
H_2O SPC/E	H	0.000	0.0000	0.4238e	[20]
	O	3.166	0.1554	-0.8476e	
O_3	O_{center}	2.896	0.2530	0.2400e	[11,16]
	O_{side}	2.896	0.2530	-0.1200e	
OH	H	0.000	0.0000	0.50e	[16]
	O	3.166	0.1554	-0.50e	
HO_2	H	0.000	0.0000	0.4454e	[16]
	O_{center}	2.626	0.4121	-0.4228e	
	O_{side}	2.626	0.4121	-0.0226e	
H_2O_2	H	0.000	0.0000	0.4976e	[16]
	O	3.166	0.1554	-0.4976e	

Table II: Aqueous bulk concentrations and their highest and averaged values in the interfacial region, compared to the gas phase value, for seven important atmospheric gases.

	Gas phase	**Aqueous bulk**	**Aqueous surface – highest value**	**Aqueous surface – averaged value**	**Width of the interfacial peak (A)**
N_2	**1.0**	**0.010**	**1.8**	**1.47**	**5.2**
O_2	**1.0**	**0.046**	**2.4**	**1.76**	**5.7**
O_3	**1.0**	**0.33**	**7.1**	**3.62**	**8.3**
OH	**1.0**	**1100**	**11000**	**8800**	**6.9**
H_2O	**1.0**	**75000**	**75000**	**75000**	**0**
HO_2	**1.0**	**90000**	**290000**	**206000**	**4.4**
H_2O_2	**1.0**	**17000000**	**34000000**	**25700000**	**3.7**

Figure Captions

Fig. 1 A graphical representation of the computational setup for the calculation of the potential of mean force.

Fig. 2 A typical force profile and the corresponding potential of mean force for moving a gas molecule across an aqueous slab the extent of which is characterized by the water density profile.

Fig. 3 A typical potential of mean force and the corresponding concentration profile for a gas molecules moving across an aqueous slab.

Fig. 4 Potential of mean force for moving a) N_2, b) O_2, c) O_3 through an aqueous slab defined via the water density profile. The experimental hydration energies obtained from the Henry's law constants in several measurements are displayed as horizontal lines.

Fig. 5 Potential of mean force for moving a) OH, b) H_2O, c) HO_2, and d) H_2O_2 through an aqueous slab defined via the water density profile. The experimental hydration energies obtained from the Henry's law constants in several measurements are displayed as horizontal lines.

Figure 1

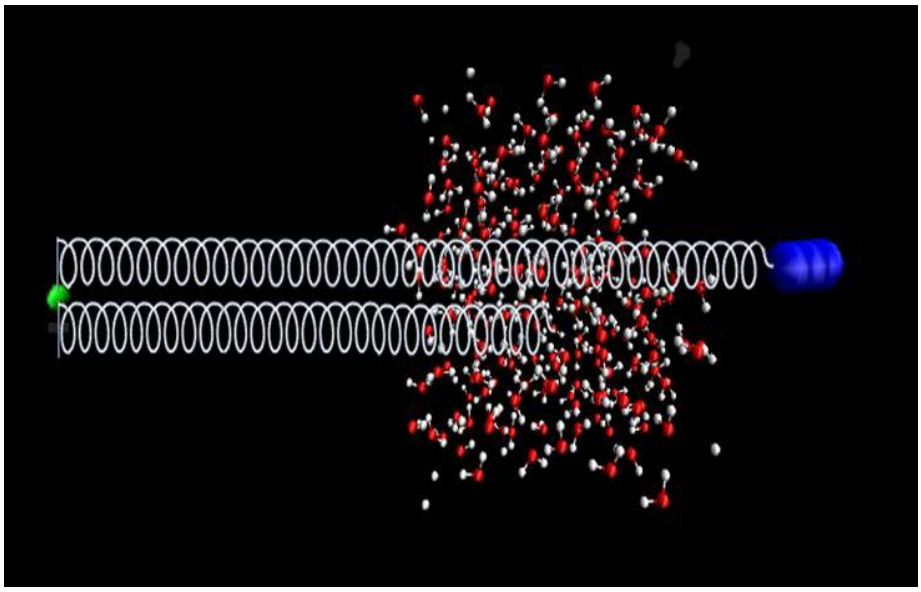

Figure 2

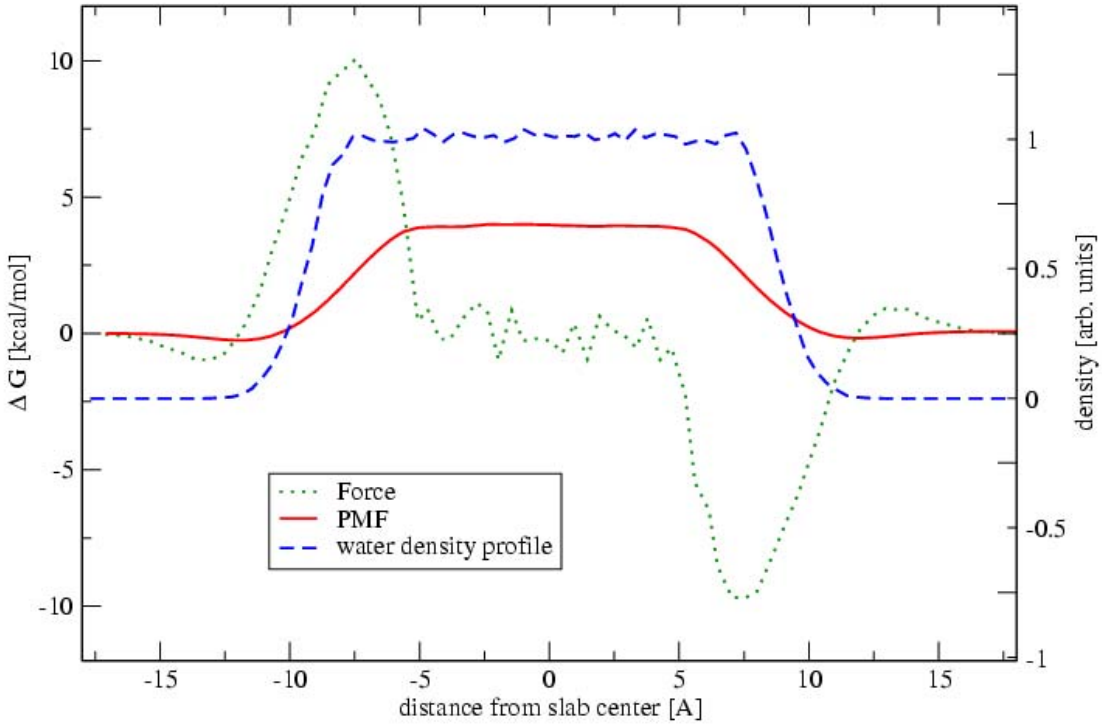
Δ G [kcal/mol]
density [arb. units]
distance from slab center [A]
Force
PMF
water density profile
10
5
0
-5
-10
1
0.5
0
-0.5
-1
-15
-10
-5
0
5
10
15

Figure 3

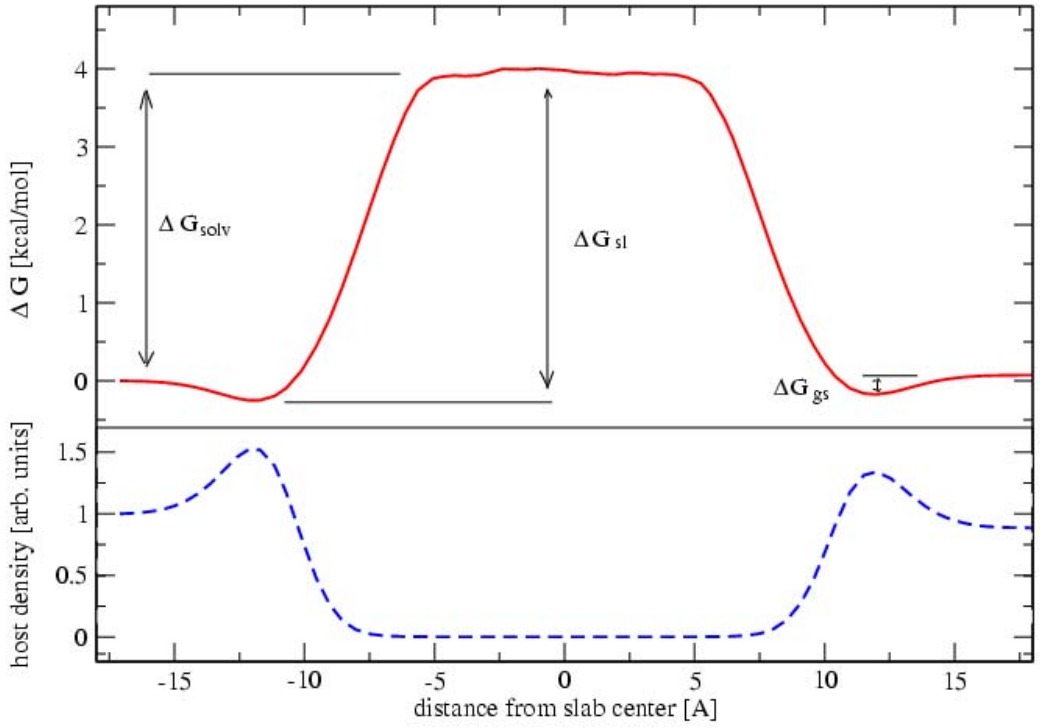
Δ G [kcal/mol]
Δ G solv
Δ G sl
ΔG gs
‡
host density [arb. units]
distance from slab center [A]

Figure 4a

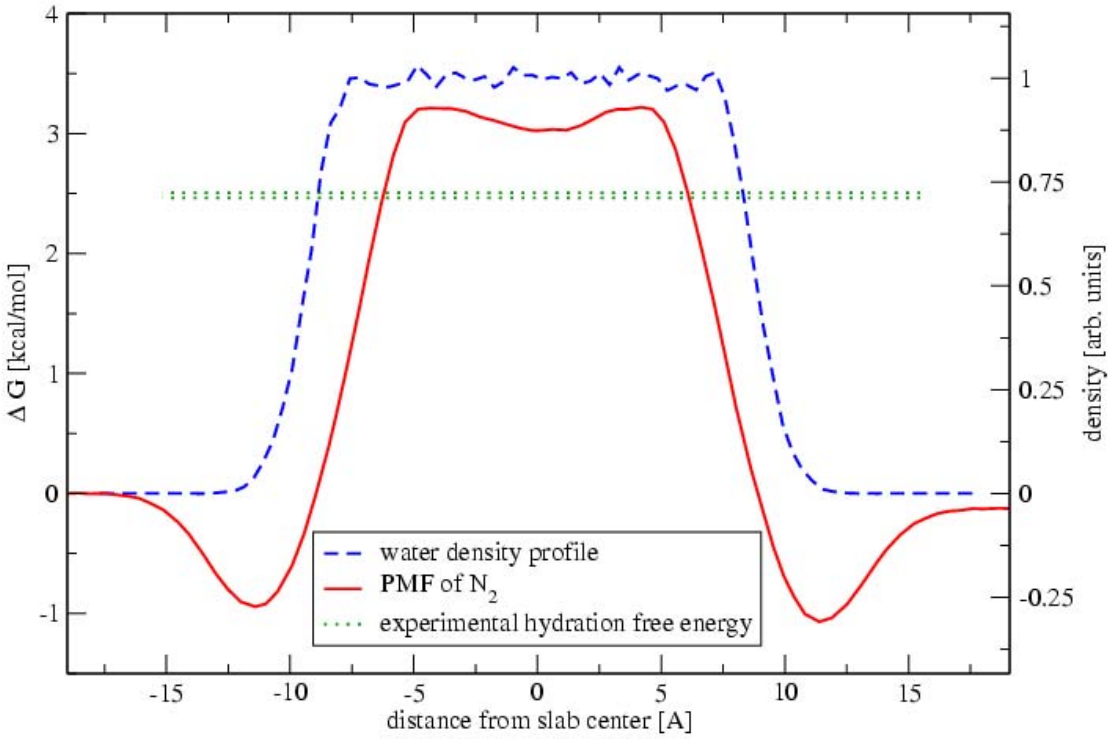
Δ G [kcal/mol]
density [arb. units]
distance from slab center [A]
water density profile
PMF of N2
experimental hydration free energy
4
3
2
1
0
-1
1
0.75
0.5
0.25
0
-0.25
-15
-10
-5
0
5
10
15

Figure 4b

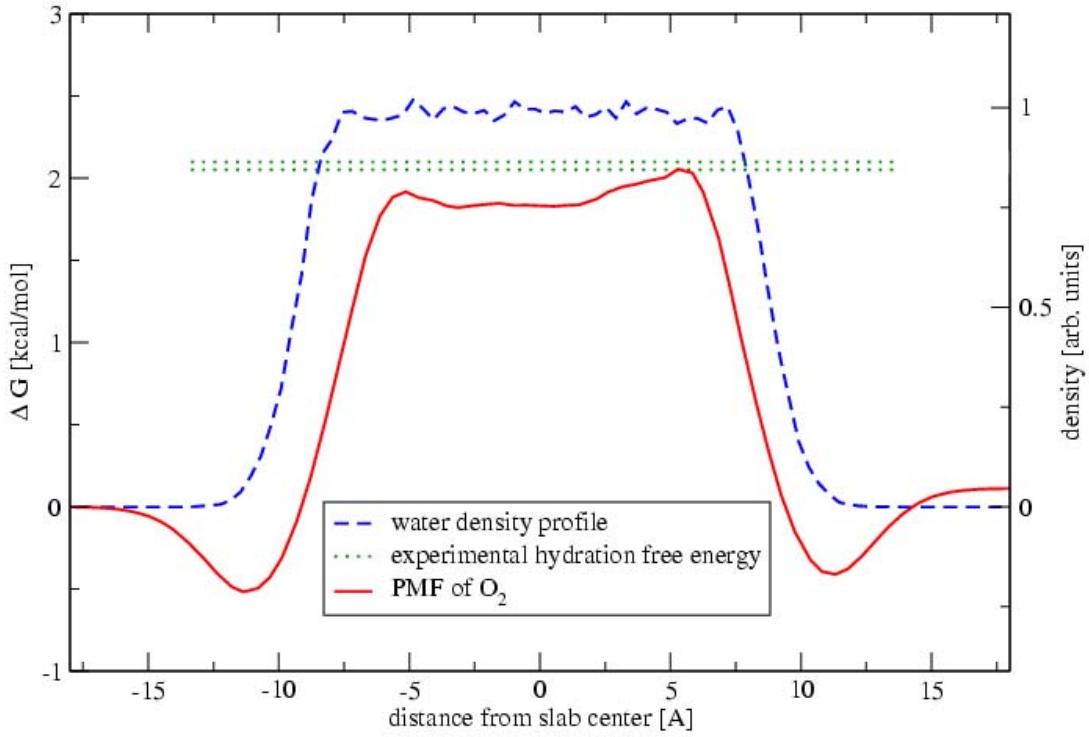
3
2
1
0
-1
Δ G [kcal/mol]
1
0.5
0
density [arb. units]
-15
-10
-5
0
5
10
15
distance from slab center [A]
water density profile
experimental hydration free energy
PMF of O2

Figure 4c

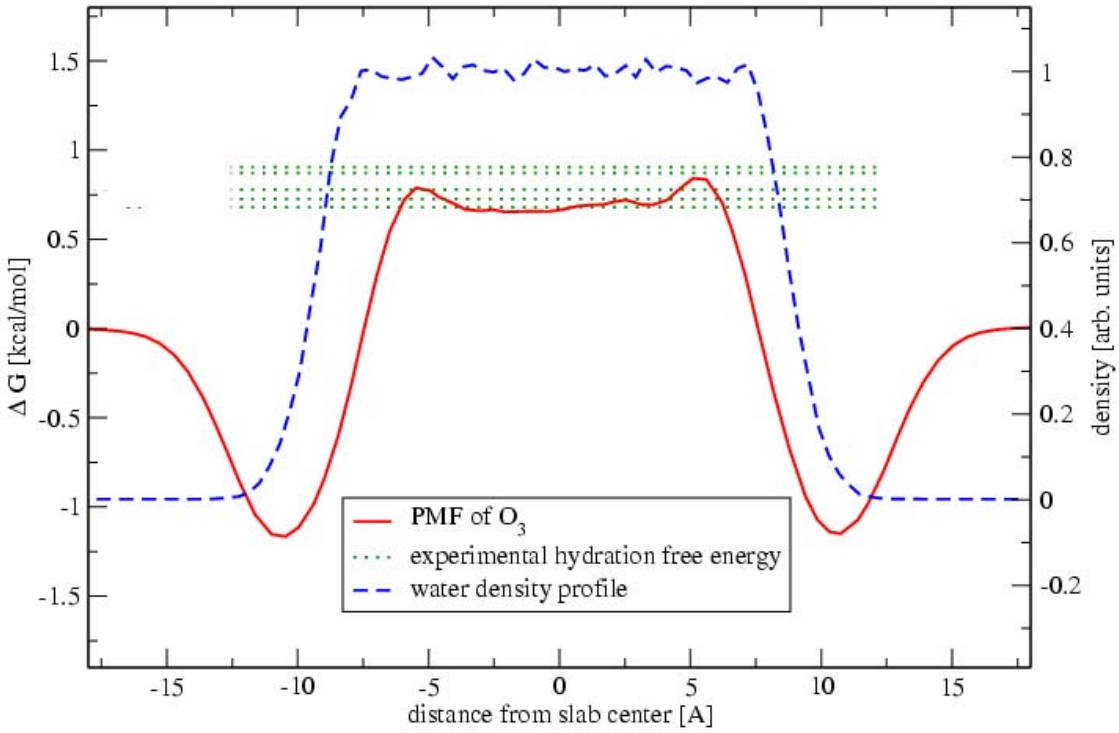
1.5
1
0.5
0
-0.5
-1
-1.5
Δ G [kcal/mol]
1
0.8
0.6
0.4
0.2
0
-0.2
density [arb. units]
-15
-10
-5
0
5
10
15
distance from slab center [A]
PMF of O3
experimental hydration free energy
water density profile

Figure 5a

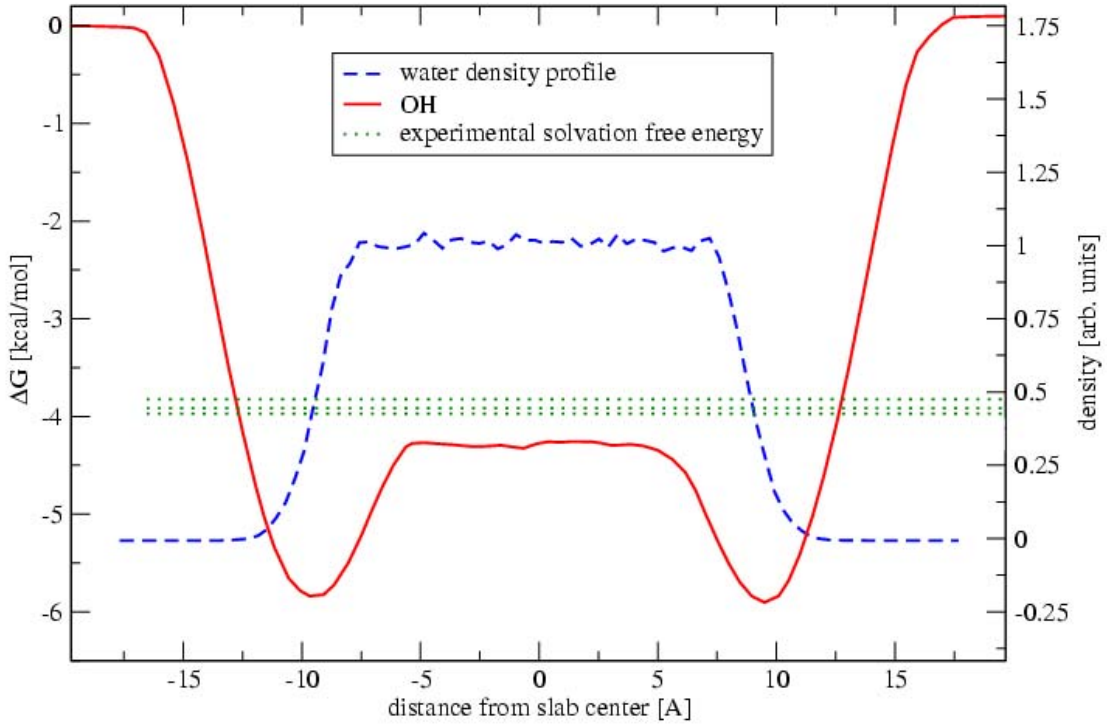
water density profile
OH
experimental solvation free energy
ΔG [kcal/mol]
density [arb. units]
distance from slab center [A]
0
-1
-2
-3
-4
-5
-6
1.75
1.5
1.25
1
0.75
0.5
0.25
0
-0.25
-15
-10
-5
0
5
10
15

Figure 5b

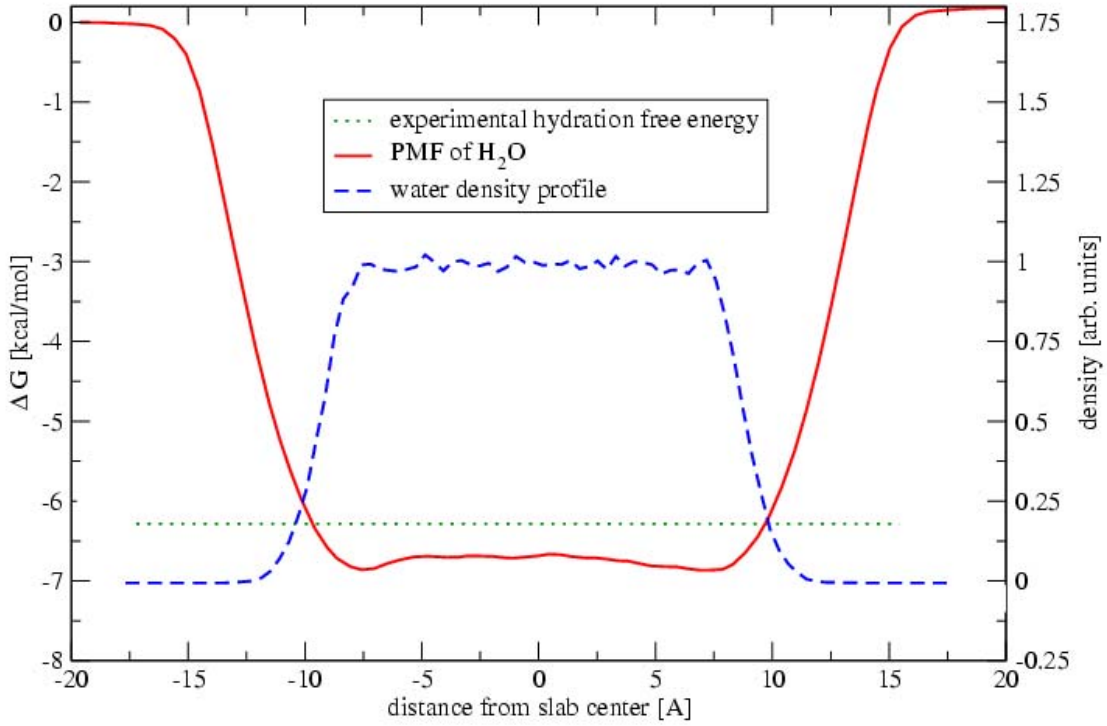
experimental hydration free energy
PMF of H_2O
water density profile
ΔG [kcal/mol]
density [arb. units]
distance from slab center [A]
0
-1
-2
-3
-4
-5
-6
-7
-8
1.75
1.5
1.25
1
0.75
0.5
0.25
0
-0.25
-20
-15
-10
-5
0
5
10
15
20

Figure 5c

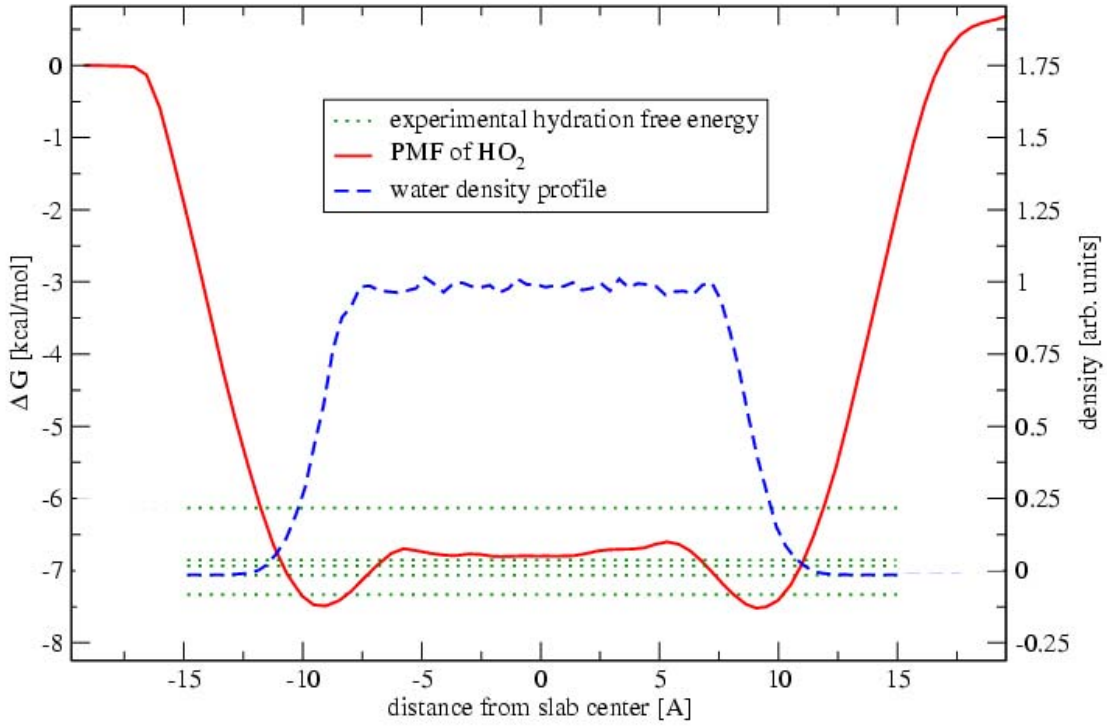
experimental hydration free energy
PMF of HO_2
water density profile
ΔG [kcal/mol]
density [arb. units]
distance from slab center [A]
0
-1
-2
-3
-4
-5
-6
-7
-8
1.75
1.5
1.25
1
0.75
0.5
0.25
0
-0.25
-15
-10
-5
0
5
10
15

Figure 5d

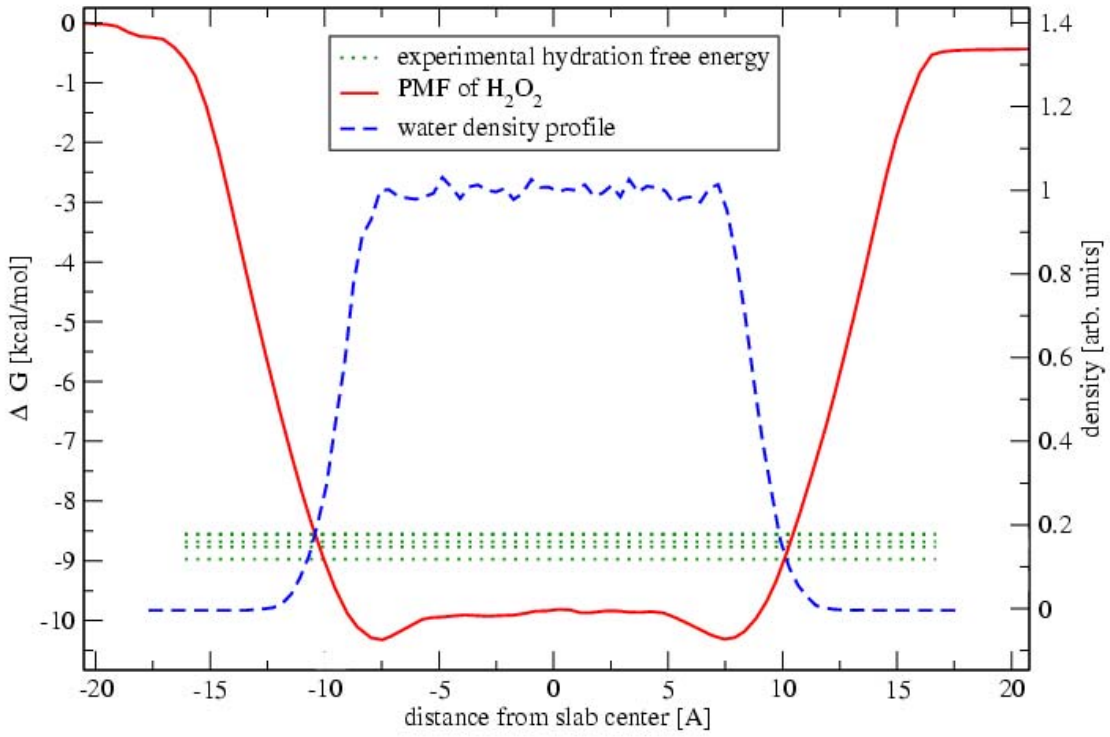
experimental hydration free energy
PMF of H_2O_2
water density profile
Δ G [kcal/mol]
density [arb. units]
distance from slab center [A]
0
-1
-2
-3
-4
-5
-6
-7
-8
-9
-10
1.4
1.2
1
0.8
0.6
0.4
0.2
0
-20
-15
-10
-5
0
5
10
15
20

References:

(1) Finlayson-Pitts, B. J.; J. N. Pitts, J. *Chemistry of the Upper and Lower Atmosphere - Theory, Experiments, and Applications*; Academic Press: San Diego, 2000.

(2) Knipping, E. M.; Lakin, M. J.; Foster, K. L.; Jungwirth, P.; Tobias, D. J.; Gerber, R. B.; Dabdub, D.; Finlayson-Pitts, B. J. *Science* **2000**, *288*, 301-306.

(3) Finlayson-Pitts, B. J. *Chem. Rev.* **2003**, *103*, 4801.

(4) Sander, R. *Surv. Geophys.* **1999**, *20*, 1.

(5) Defay, R.; Prigogine, I. *Surface tension and adsorption*; Wiley: New York, 1966.

(6) Djikaev, Y. S.; Tabazadeh, A. *J. Geophys. Res.-Atmos.* **2003**, *108*, 4689.

(7) Hamad, S.; Lago, S.; Mejias, J. A. *J. Phys. Chem. A* **2002**, *106*, 9104.

(8) Cooper, P. D.; Kjaergaard, H. G.; Langford, V. S.; McKinley, A. J.; Quickenden, T. I.; Schofield, D. P. *J. Am. Chem. Soc.* **2003**, *125*, 6048.

(9) Belair, S. D.; Hernandez, H.; Francisco, J. S. *J. Am. Chem. Soc.* **2004**, *126*, 3024.

(10) Shi, Q. C.; Belair, S. D.; Francisco, J. S.; Kais, S. *Proc. Nat. Acad. Sci.* **2003**, *100*, 9686.

(11) Roeselova, M.; Jungwirth, P.; Tobias, D. J.; Gerber, R. B. *J. Phys. Chem. B* **2003**, *107*, 12690.

(12) Roeselova, M.; Vieceli, J. S.; Dang, L. X.; Tobias, D. J. *J. Am. Chem. Soc.* **2004**, *submitted*.

(13) Morita, A.; Kanaya, Y.; Francisco, J. S. *J. Geophys. Res.-Atmos* **2004**, *109*, 09201.

(14) Dang, L. X.; Garrett, B. C. *Chem. Phys. Lett.* **2004**, *385*, 309.

(15) Bader, J. S.; Chandler, D. *J. Phys. Chem.* **1992**, *96*, 6423.

(16) Lindahl, E.; Hess, B.; van der Spoel, D. *J. Molec. Modeling* **2001**, *7*, 306.

(17) Bennaim, A.; Marcus, Y. *J. Chem. Phys.* **1984**, *81*, 2016.

(18) Sander, R. “Compilation of Henry's Law Constants for Inorganic and Organic Species of Potential Importance in Environmental Chemistry (Version 3), www.mpch-mainz.mpg.de/~sander/res/henry.html,”, 1999.

(19) Essmann, U.; Perera, L.; Berkowitz, M. L.; Darden, T.; Lee, H.; Pedersen, L. G. *J. Chem. Phys.* **1995**, *103*, 8577.

(20) Berendsen, H. J. C.; Grigera, J. R.; Straatsma, T. P. *J. Phys. Chem.* **1987**, *91*, 6269.

(21) Jordan, P. C.; Vanmaaren, P. J.; Mavri, J.; Vanderspoel, D.; Berendsen, H. J. C. *J. Chem. Phys.* **1995**, *103*, 2272.

(22) M. J. Frisch, G. W. T., H. B. Schlegel, G. E. Scuseria, M. A. Robb, J. R. Cheeseman, J. A. Montgomery, Jr., T. Vreven, K. N. Kudin, J. C. Burant, J. M. Millam, S. S. Iyengar, J. Tomasi, V. Barone, B. Mennucci, M. Cossi, G. Scalmani, N. Rega, G. A. Petersson, H. Nakatsuji, M. Hada, M. Ehara, K. Toyota, R. Fukuda, J. Hasegawa, M. Ishida, T. Nakajima, Y. Honda, O. Kitao, H. Nakai, M. Klene, X. Li, J. E. Knox, H. P. Hratchian, J. B. Cross, C. Adamo, J. Jaramillo, R. Gomperts, R. E. Stratmann, O. Yazyev, A. J. Austin, R. Cammi, C. Pomelli, J. W. Ochterski, P. Y. Ayala, K. Morokuma, G. A. Voth, P. Salvador, J. J. Dannenberg, V. G. Zakrzewski, S. Dapprich, A. D. Daniels, M. C. Strain, O. Farkas, D. K. Malick, A. D. Rabuck, K. Raghavachari, J. B. Foresman, J. V. Ortiz, Q. Cui, A. G. Baboul, S. Clifford, J. Cioslowski, B. B. Stefanov, G. Liu, A. Liashenko, P. Piskorz, I. Komaromi, R. L. Martin, D. J. Fox, T. Keith, M. A. Al-Laham, C. Y. Peng, A. Nanayakkara, M. Challacombe, P. M. W. Gill, B. Johnson, W. Chen, M. W. Wong, C. Gonzalez, and J. A. Pople Pittsburgh PA, 2003.

(23) Taylor, R. S.; Ray, D.; Garrett, B. C. *J. Phys. Chem. B* **1997**, *101*, 5473.

(24) Jayne, J. T.; Davidovits, P.; Worsnop, D. R.; Zahniser, M. S.; Kolb, C. E. *J. Phys. Chem.* **1990**, *94*, 6041.

(25) Hu, J. H.; Shi, Q.; Davidovits, P.; Worsnop, D. R.; Zahniser, M. S.; Kolb, C. E. *J. Phys. Chem.* **1995**, *99*, 8768.

(26) Donaldson, D. J.; Guest, J. A.; Goh, M. C. *J. Phys. Chem.* **1995**, *99*, 9313.

(27) Hanson, D. R.; Ravishankara, A. R. *J. Phys. Chem.* **1994**, *98*, 5728.

(28) George, C.; Behnke, W.; Scheer, V.; Zetzsch, C.; Magi, L.; Ponche, J. L.; Mirabel, P. *Geophys. Res. Lett.* **1995**, *22*, 1505.

(29) Boniface, J.; Shi, Q.; Li, Y. Q.; Cheung, J. L.; Rattigan, O. V.; Davidovits, P.; Worsnop, D. R.; Jayne, J. T.; Kolb, C. E. *J. Phys. Chem. A* **2000**, *104*, 7502.

(30) Clegg, S. M.; Abbatt, J. P. D. *J. Phys. Chem. A* **2001**, *105*, 6630.

(31) Katrib, Y.; Deiber, G.; Schweitzer, F.; Mirabel, P.; George, C. *J. Aerosol Sci.* **2001**, *32*, 893.

(32) Strekowski, R. S.; Remorov, R.; George, C. *J. Phys. Chem. A* **2003**, *107*, 2497.

(33) Tabazadeh, A.; Yokelson, R. J.; Singh, H. B.; Hobbs, P. V.; Crawford, J. H.; Iraci, L. T. *Geophys. Res. Lett.* **2004**, *31*, 06114.

(34) Hobbs, P. V.; Sinha, P.; Yokelson, R. J.; Christian, T. J.; Blake, D. R.; Gao, S.; Kirchstetter, T. W.; Novakov, T.; Pilewskie, P. *J. Geophys. Res.-Atmos.* **2003**, *108*, 8485.

(35) Elliot, A. J.; McCracken, D. J. *Radiat. Phys. Chem.* **1989**, *33* 69. NIST In *NIST Standard Reference Database 40*, 2004.

(36) Donaldson, D. J.; Anderson, D. *J. Phys. Chem. A* **1999**, *103*, 871.

(37) Mmereki, B. T.; Donaldson, D. J. *J. Phys. Chem. A* **2003**, *107*, 11038.

(38) Mmreki, B. T.; Donaldson, D. J.; Gilman, J. B.; Eliason, T. L.; Vaida, V. *Atmos. Env.*, *submitted.*

(39) Tervahattu, H.; Hartonen, K.; Kerminen, V. M.; Kupiainen, K.; Aarnio, P.; Koskentalo, T.; Tuck, A. F.; Vaida, V. *J. Geophys. Res.-Atmos.* **2002**, *107*, 4053.

(40) Tervahattu, H.; Juhanoja, J.; Kupiainen, K. *J. Geophys. Res.-Atmos.* **2002**, *107*, 4319.

(41) Salvador, P.; Curtis, J. E.; Tobias, D. J.; Jungwirth, P. *Phys. Chem. Chem. Phys.* **2003**, *5*, 3752.

(42) Raja, S.; Valsaraj, K. T. *Env. Sci. Tech.* **2004**, *38*, 763.

(43) Jayne, J. T.; Gardner, J. A.; Davidovits, P.; Worsnop, D. R.; Zahniser, M. S.; Kolb, C. E. *J. Geophys. Res.-Atmos.* **1990**, *95*, 20559.